

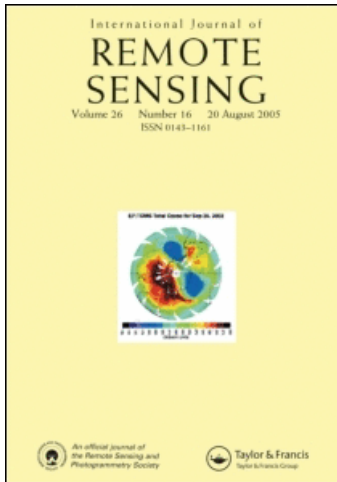
This article was downloaded by: [Universidad de Valencia]

On: 10 November 2008

Access details: Access Details: [subscription number 779262402]

Publisher Taylor & Francis

Informa Ltd Registered in England and Wales Registered Number: 1072954 Registered office: Mortimer House, 37-41 Mortimer Street, London W1T 3JH, UK



## International Journal of Remote Sensing

Publication details, including instructions for authors and subscription information:

<http://www.informaworld.com/smpp/title-content=t713722504>

### Validation of a temperature emissivity separation hybrid method from airborne hyperspectral scanner data and ground measurements in the SEN2FLEX field campaign

L. F. Peres <sup>ab</sup>; J. A. Sobrino <sup>c</sup>; R. Libonati <sup>ab</sup>; J. C. Jiménez-Muñoz <sup>c</sup>; C. C. Dacamara <sup>b</sup>; M. Romaguera <sup>c</sup>

<sup>a</sup> Instituto Nacional de Pesquisas Espaciais - Centro de Previsão de Tempo e Estudos Climáticos - Rod. Pres Dutra, Cachoeira Paulista/SP, Brazil <sup>b</sup> University of Lisbon, CGUL, IDL, Campo Grande, 1749-016, Lisbon, Portugal <sup>c</sup> Global Change Unit, Department of Thermodynamics, Faculty of Physics, University of Valencia, 46100, Burjassot, Spain

First Published: December 2008

**To cite this Article** Peres, L. F., Sobrino, J. A., Libonati, R., Jiménez-Muñoz, J. C., Dacamara, C. C. and Romaguera, M. (2008) 'Validation of a temperature emissivity separation hybrid method from airborne hyperspectral scanner data and ground measurements in the SEN2FLEX field campaign', *International Journal of Remote Sensing*, 29:24, 7251 — 7268

**To link to this Article:** DOI: 10.1080/01431160802036532

**URL:** <http://dx.doi.org/10.1080/01431160802036532>

PLEASE SCROLL DOWN FOR ARTICLE

Full terms and conditions of use: <http://www.informaworld.com/terms-and-conditions-of-access.pdf>

This article may be used for research, teaching and private study purposes. Any substantial or systematic reproduction, re-distribution, re-selling, loan or sub-licensing, systematic supply or distribution in any form to anyone is expressly forbidden.

The publisher does not give any warranty express or implied or make any representation that the contents will be complete or accurate or up to date. The accuracy of any instructions, formulae and drug doses should be independently verified with primary sources. The publisher shall not be liable for any loss, actions, claims, proceedings, demand or costs or damages whatsoever or howsoever caused arising directly or indirectly in connection with or arising out of the use of this material.

## Validation of a temperature emissivity separation hybrid method from airborne hyperspectral scanner data and ground measurements in the SEN2FLEX field campaign

L. F. PERES\*<sup>†‡</sup>, J. A. SOBRINO<sup>§</sup>, R. LIBONATI<sup>†‡</sup>, J. C. JIMÉNEZ-MUÑOZ<sup>§</sup>,  
C. C. DACAMARA<sup>‡</sup> and M. ROMAGUERA<sup>§</sup>

<sup>†</sup>Instituto Nacional de Pesquisas Espaciais – Centro de Previsão de Tempo e Estudos Climáticos – Rod. Pres Dutra, km 39, CEP 12630-000, Cachoeira Paulista/SP, Brazil

<sup>‡</sup>University of Lisbon, CGUL, IDL, Campo Grande, Ed C8, Piso 6, 1749-016, Lisbon, Portugal

<sup>§</sup>Global Change Unit, Department of Thermodynamics, Faculty of Physics, University of Valencia, Dr. Moliner 50, 46100, Burjassot, Spain

(Received 16 December 2006; in final form 30 September 2007)

This paper presents an assessment of the performance of a hybrid method that allows a simultaneous retrieval of land-surface temperature (LST) and emissivity (LSE) from remotely-sensed data. The proposed method is based on a synergistic usage of the split-window (SW) algorithm and the two-temperature method (TTM) and combines the advantages of both procedures while mitigating their drawbacks. The method was implemented for thermal channels 76 (10.56  $\mu\text{m}$ ) and 78 (11.72  $\mu\text{m}$ ) of the Airborne Hyperspectral Scanner (AHS), which was flown over the Barrax test site (Albacete, Spain) in the second week of July 2005, within the framework of the Sentinel-2 and Fluorescence Experiment (SEN2FLEX) field campaign. A set of radiometric measurements was performed in the thermal infrared region in coincidence with aircraft overpasses for different surface types, e.g. bare soil, water body, corn, wheat, grass. The hybrid method was tested and compared with a standard SW algorithm and the results obtained show that the hybrid method is able to provide better estimates of LST, with values of bias (RMSE) of the order of 0.8 K (1.9 K), i.e. about one third (one half) of the corresponding values of 2.7 K (3.4 K) that were obtained for bias (RMSE) when using the SW algorithm. These figures provide a sound indication that the developed hybrid method is particularly useful for surface and atmospheric conditions where SW algorithms cannot be accurately applied.

### 1. Introduction

Land-surface temperature (LST) is an important parameter for understanding land–atmosphere interactions because it is sensitive to the partitioning of energy and mass fluxes at the Earth’s surface. Instruments on-board Earth observation satellites and working in the thermal infrared (TIR) spectrum are currently expected to provide measurements of LST on a global basis with uniformity and continuity at spatial and temporal resolutions that are suitable for most modelling applications.

Problems encountered in estimating LST from TIR remote sensing data mainly relate to the fact that radiance measured is not only affected by LST, but also by

---

\*Corresponding author. Email: lperes@cptec.inpe.br

land-surface emissivity (LSE), as well as by the thermal structure and composition of the atmosphere. Therefore, an accurate retrieval of LST from space data requires a proper characterization of the atmospheric influence as well as a distinction between the effects of LST and LSE. However, even considering the special case of a perfect homogeneous, isothermal and smooth surface, and assuming that the signal has been corrected from all atmospheric influences, a single TIR measurement leads to a number of equations that is always less than the number of unknowns. Therefore, a unique solution to the problem of LST inversion/retrieval cannot be obtained if based on radiative data alone. (Peres and DaCamara 2004). Accordingly, there is the need for *a priori* complementary information in order to recover both parameters uniquely, and the developed techniques differ according to the required closing assumptions.

For instance, split-window (SW) algorithms assume that LSE is known *a priori* in order to close the system of equations. In this case, the task becomes easier because the nature of the problem is deterministic and the SW method essentially reduces to performing an atmospheric correction for known LSE, which is based on the differential absorption in two adjacent TIR bands within the same atmospheric window. Several formulations have been derived with different levels of refinement, where LST is in general expressed by means of linear combinations of brightness temperature (BT) of the two adjacent bands. Besides their simplicity and computational efficiency the main advantage of SW algorithms is that radio-sounding measurements are not required to perform the atmospheric correction. However, different authors (e.g. Becker 1987, Wan and Dozier 1996) have shown that the main drawback of SW algorithms is that large errors on LST may arise due to uncertainties in LSE and therefore their ability to accurately retrieve LST crucially depends on an adequate *a priori* knowledge of LSE. In fact over areas where LSE is highly variable and not well known *a priori* the use of SW algorithms is inadequate, raising the need for methods that allow LST to be retrieved without a direct knowledge of LSE.

On the other hand, the two-temperature method (TTM) does not strictly assume an *a priori* knowledge of LSE allowing a simultaneous retrieval of LST and LSE if the surface is observed at two different temperatures at least and LSE does not change between observations. Such types of method are usually referred to in the literature as emissivity-temperature separation algorithms and the common characteristics (and drawbacks) are the requirement of accurate temperature and humidity atmospheric profiles as inputs to a radiative transfer model (RTM) in order to perform the atmospheric correction. In this respect, Peres and DaCamara (2004) have assessed the performance of TTM by taking into consideration instrument performance (i.e. radiometric noise), as well as errors in the atmospheric profiles. Results suggest that TTM may be used as a complementary method for LST retrievals in those areas where LSE is not well known *a priori*, but there is the limitation due to the fact that the used optimization approach imposes substantial mathematical and numerical requirements (e.g. the use of different initial guess vectors), which may prevent the method becoming operational over large areas.

In order to circumvent the main drawbacks of both above-mentioned methods, we have proposed a new hybrid procedure that is based on a synergistic use of SW and TTM (Peres and DaCamara 2008), and the goal is to combine the most attractive features of both methods while mitigating some of the pitfalls.

This work assesses the accuracy of the developed hybrid method and compares its performance with a standard SW algorithm. The study was performed using data from the Airborne Hyperspectral Scanner (AHS) and ground-based measurements acquired in the framework of the Sentinel-2 and Fluorescence Experiment (SEN2FLEX) field campaign.

## 2. Field data

The SEN2FLEX is a campaign combining different activities related on the one hand to experiments for the observation of solar induced fluorescence signal over multiple surface targets (AIRFLEX) and on the other to the monitoring of terrestrial surfaces and their evolution in time (Sentinel-2). The Sentinel-2 initiative is carried out in the framework of the Global Monitoring for Environment and Security (GMES) programme and consists of a European polar orbit satellite system, currently under development by the European Space Agency (ESA), which combines high and low resolution superspectral imagers. The Sentinel-2 mission will ensure the continuation of SPOT-type measurements (including Vegetation), Envisat/MERIS for terrestrial applications and Landsat/ETM+ (<http://www.uv.es/leo/sen2flex/>). The field campaign was conducted in the Barrax test site (Albacete, Spain) in July 2005, an agricultural area within La Mancha, a plateau 700 m above sea level. The test site is located in the west part of the province of Albacete (coordinates 30°3' N, 2°6' W) and the area is characterized by a flat morphology and large, uniform land-use units, with differences in elevation ranging up to 2 m. The region consists of approximately 65% dry and 35% irrigated land with different types of crop fields and orchards (figure 1).

Temperature measurements in the SEN2FLEX field campaign were made over the Barrax test site on 12, 13 and 14 July 2005 using different field thermal radiometers (e.g. OPTRIS, RAYTEK ST6, RAYTEK MID, CIMEL CE 312-1 and CIMEL CE 312-2 ASTER). The main technical characteristics of the thermal radiometers, the heights of the radiometers above the targets and the resulting diameter circular footprints are given in table 1. Accordingly, measurements were performed from nadir at 1.5 m and 2.5 m heights using six thermal radiometers with different fields of view (FOVs) providing a diameter circular footprint between 0.05 m and 1.31 m (see table 1). It is worth mentioning that two blackbodies (EVEREST 1000 and GALAI 204-P) were used for calibration purposes. In addition, a goniometer with a rotating arm installed to change the observation angle in the zenith direction and a half circle roadway to change the observation angle in the azimuth direction was used to measure directional brightness temperature. It is important to mention at this point that the investigation of the angular variation of the infrared radiation is beyond the scope of this paper and therefore only measurements from nadir were used in the present study. Transects were realized over selected surfaces concurrently to the AHS flights (see table 2), starting half an hour before and ending half an hour after. Thermal measurements were also continuously recorded with radiometers located on fixed masts over selected areas and periods of time. The LSE of representative samples was measured by means of the Box method (Nerry *et al.* 1990) and by using the CIMEL CE312-2 radiometer together with the temperature-emissivity separation (TES) algorithm (Gillespie *et al.* 1999). Figure 2 shows the location of the different parcels where the measurements were carried out and the validation was performed.

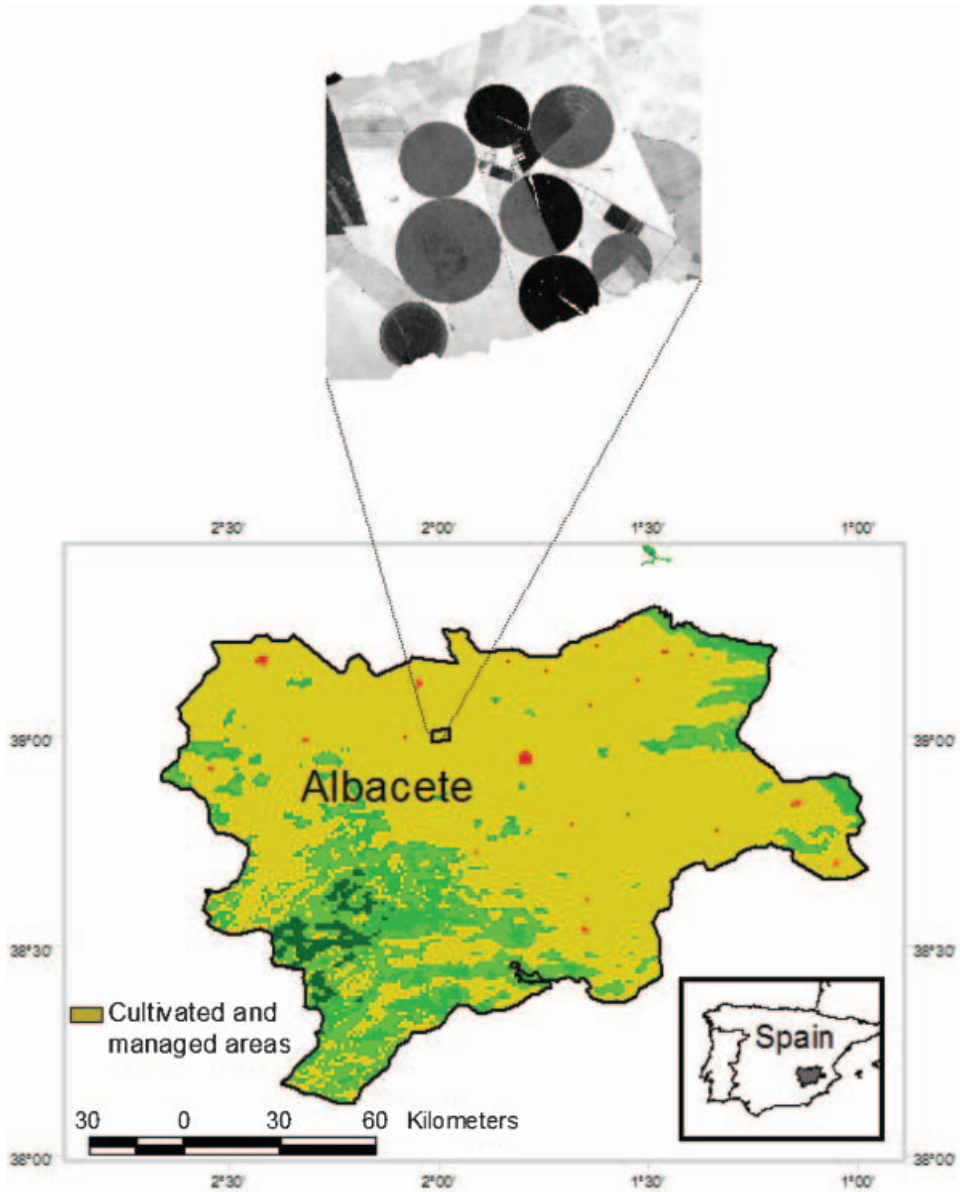


Figure 1. The Barrax test site in the province of Albacete, Spain, and the main vegetation types, as defined by the GLC2000 Land Cover map.

The AHS is an imaging 80-band line-scanner radiometer (developed by Sensytech Inc, currently Argon ST, Fairfax, VA, USA) and operated by INTA (Spanish Institute for Aerospace Technology). It is based on previous airborne hyperspectral scanners such as MIVIS (Multispectral Infrared and Visible Imaging Spectrometer) and MAS (MODIS Airborne Simulator). This instrument has been installed in the INTA's aircraft (CASA 212-200 N/S 270, *Paternina*) and during the AHS remote sensing surveys, position and altitude measurements were provided by an Applanix POS AV 410 installed on top of the AHS. Tables 3 and 4 show the AHS technical

Table 1. Technical characteristics of the thermal radiometers, the heights of the radiometers and the resulting diameter circular footprints.

Model	Bands ( $\mu\text{m}$ )	Range ( $^{\circ}\text{C}$ )	Accuracy ( $^{\circ}\text{C}$ )	FOV ( $^{\circ}$ )	Height (m)	Diameter (m)
CIMEL CE 312-1	8–13 8.2–9.2 10.3–11.3 11.5–12.5	–80 to 60	0.1	10	1.5	0.26
CIMEL CE 312-2	8–13 11.0–11.7 10.3–11.0 8.9–9.3 8.5–8.9 8.1–8.5	–80 to 60	0.1	10	1.5	0.26
OPTRIS	8–14	–32 to 530	1.0	3	1.5	0.08
RAYTEK ST6 Standard	8–14	–32 to 400	1.0	7	1.5	0.18
RAYTEK ST6 ProPlus	8–14	–32 to 400	1.0	2	1.5	0.05
RAYTEK MID	8–14	–40 to 600	1.0	30	1.5–2.5	0.78–1.31

Table 2. Date and time (UTM) of the Airborne Hyperspectral Scanner (AHS) flights.

12 July 2005		13 July 2005		14 July 2005	
$t_1$	$t_2$	$t_1$	$t_2$	$t_1$	$t_2$
12:21	22:32	08:15	12:09	08:23	12:25

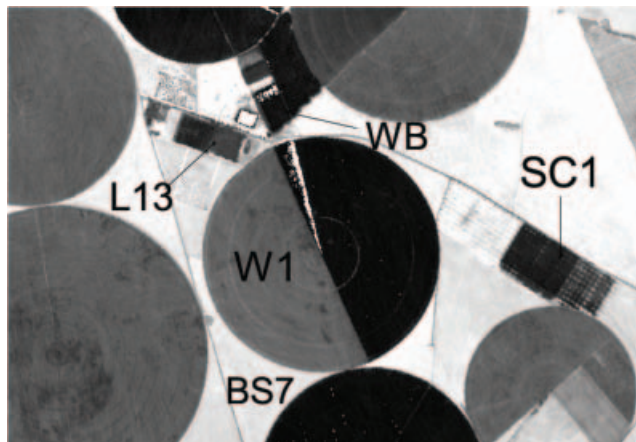


Figure 2. The study area of Barrax showing the location and land cover types of parcels where comparisons were performed. L13 is grass, WB is water, W1 is wheat, BS7 is bare soil and SC1 is corn. The image corresponds to Airborne Hyperspectral Scanner (AHS) band 76 ( $10.56\ \mu\text{m}$ ) raw data and it was acquired on 12 July 2005 at 12:21 UTM, with a pixel size of 3.4 m.

specifications and the arrangement of the spectral bands, respectively. It is worth noting that AHS bands 71–80 in the long-wave infrared (LWIR) port completely cover the atmospheric window ( $8.2\text{--}12.9\ \mu\text{m}$ ) and therefore AHS is a very powerful instrument for thermal remote sensing (Alix *et al.* 2005). The spectral characteristics of bands 71–80 are displayed in figure 3, where the corresponding filter functions

Table 3. Technical specifications of the Airborne Hyperspectral Scanner (AHS) instrument.

FOV	90° ( $\pm 45^\circ$ )
IFOV	2.5 mrad
GFOV	2–6 m at 140 kts platform speed
Scan rate	6.25, 12.5, 18.75, 25, 31.25, 35 rps
Digitisation accuracy	12 bits
Pixels per scanline	750
Reference sources	Two controllable thermal blackbodies (15°C and 55°C)

Table 4. Arrangement of the Airborne Hyperspectral Scanner (AHS) spectral bands.

Optical port	Channels	Spectral region ( $\mu\text{m}$ )
1 (VIS/NIR)	1–20	0.44–1.65
2 (SWIR)	21–63	2.02–2.50
3 (MWIR)	64–70	3.03–5.41
4 (LWIR)	71–80	7.95–13.17

were plotted. The AHS data used in the present work were acquired from flights at an altitude of 1340 m, yielding a pixel resolution of 3.4 m (for a description of the AHS flight parameters, see table 5).

Knowledge of the atmospheric conditions, mainly from humidity and temperature profiles, is required to perform accurate atmospheric corrections of satellite/airborne imagery. Accordingly, free atmospheric soundings were performed

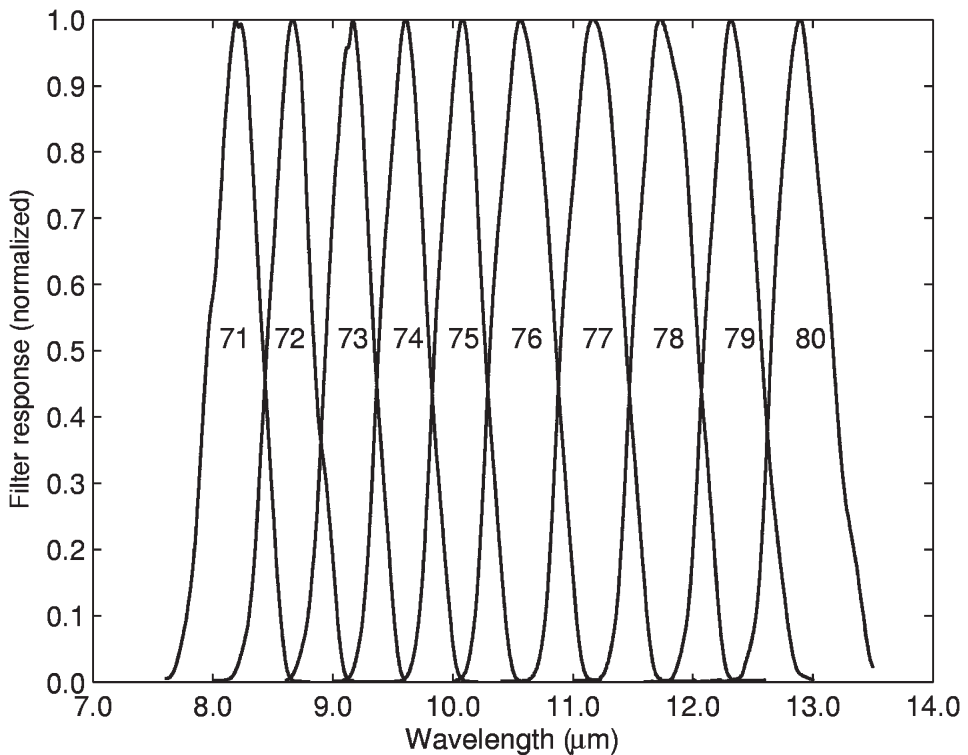


Figure 3. Filter functions for the Airborne Hyperspectral Scanner (AHS) bands located in the long-wave infrared (LWIR) port.

Table 5. Airborne Hyperspectral Scanner (AHS) flight parameters.

Flight parameters	AHS nominal (altitude m)
FOV/IFOV	90°/2.5 mrad
Flight high above terrain	1370 m
Nadir GIFOV	3.4 m
Ground sampling distance	2.9 m
Scan speed	25 rps
Inertial navigation system	Applanix POS/AV 410
Black body thermal reference	10°C/50°C

simultaneously to the AHS overpass in order to characterize the atmospheric state at Barrax during the SEN2FLEX. The Vaisala RS80 radiosondes used are small sensors integrated in a light box and released into the atmosphere on meteorological helium filled balloons. Pressure, temperature and humidity were measured at regular intervals and transmitted to the surface by radio signals. The equipment was completed with a ground station AIR Inc. TS-2AR Receiver s/n 259 for the signal reception. The atmospheric correction of the AHS thermal channels was performed based on humidity and temperature profiles from performed radiosounding measurements, which were used as input to MODTRAN4 (Berk *et al.* 2000).

### 3. Method

TTM allows for a simultaneous retrieval of LST and LSE if the surface is observed at least at two different temperatures. The method assumes that LSE does not change between observations and that atmospheric effects may be adequately estimated by means of a RTM. Assuming the Earth's surface as a Lambertian emitter–reflector and neglecting atmospheric scattering, the radiance recorded under a zenith angle  $\theta$  in a given channel  $c$  may be represented by the radiative transfer equation (RTE)

$$L_{\text{RTE}_c}(\theta) = \varepsilon_c B_c(T_s) \tau_c(\theta) + L_c^\uparrow(\theta) + L_c^\downarrow(1 - \varepsilon_c) \tau_c(\theta) \quad (1)$$

where  $\varepsilon_c$ ,  $B_c(T_s)$ ,  $\tau_c(\theta)$ ,  $L_c^\uparrow(\theta)$  and  $L_c^\downarrow$ , respectively denote the LSE, the emitted radiance given by Planck's function for the surface temperature  $T_s$ , the atmospheric transmittance, and the atmospheric upwards and downwards radiances. Assuming that a pair of observations is available (performed at times  $t_1$  and  $t_2$  in two AHS channels  $c_1$  and  $c_2$ ) then the four unknown surface parameters (i.e.  $T_s$  at times  $t_1$  and  $t_2$ , and  $\varepsilon$  in channels  $c_1$  and  $c_2$ ) may be obtained by solving a system of four equations, each one of the form given by equation (1). Following previous studies (Faysash and Smith 2000, Peres and DaCamara 2004), a quasi-Newton optimization method (Gill *et al.* 1983) was used in order to find the unknowns that minimize the cost function  $f$  given by the sum of squared differences between radiances  $L_{\text{OBS}}$  (observed radiances) and  $L_{\text{RTE}}$  (computed radiances by means of the RTE model as given by equation (1))

$$f = \sum_{\substack{c=c_1, c_2 \\ t=t_1, t_2}} \left( L_{\text{OBS}_c}^t(\theta) - L_{\text{RTE}_c}^t(\theta) \right)^2 \quad (2)$$

The hybrid procedure we have proposed consists of combining the use of *a priori* knowledge on LSE together with LST estimates as obtained from a SW algorithm. The aim is to define narrower and more reliable ranges of admissible solutions before applying TTM (figure 4) and the rationale is to increase the efficiency of

TTM from a computational point of view and especially to improve the quality of LST retrievals over areas where LSE is not well known *a priori*. Accordingly, the hybrid method procedure consists of the following three steps:

- (1) Use as input  $LSE_M$  directly from LSE maps and apply SW to obtain  $LST_{SW}$ .
- (2) Define the set of admissible solutions for TTM as  $LST_{SW} \pm 3.0$  K and  $LSE_M \pm 0.02$  where 3.0 K and 0.02 represent the assumed uncertainties of SW and LSE maps.
- (3) Search LST and LSE combination that minimizes equation (2).

In this paper  $LST_{SW}$  is given by the SW algorithm developed by Sobrino and Raissouni (2000).

$$T_s = a_0 + a_1 T_{c_1} + a_2 (T_{c_1} - T_{c_2}) + a_3 (T_{c_1} - T_{c_2})^2 + a_4 (1 - \varepsilon) + a_5 \Delta \varepsilon \quad (3)$$

where  $T_{c_1}$  ( $T_{c_2}$ ) is the brightness temperature in AHS channels  $c_1$  ( $c_2$ ),  $\varepsilon = (\varepsilon_{c_1} + \varepsilon_{c_2})/2$  is the average emissivity in AHS channels  $c_1$  and  $c_2$ ,  $\Delta \varepsilon = (\varepsilon_{c_1} - \varepsilon_{c_2})$  is the emissivity difference between the two channels, and  $a_k$  ( $k=0$  to 5) are SW coefficients estimated by means of a simulation procedure as described in §4.

## 4. Results and analyses

### 4.1 Split-window and emissivity

In order to obtain *a priori* estimates of LST from SW the algorithm (equation (3)), we have estimated the SW coefficients by means of regression analysis of simulated observed radiances as obtained from MODTRAN4. Accordingly, the following cases were considered in the simulation:

- (1) *Atmospheric temperature and humidity profiles*: The database relies upon atmospheric temperature and humidity profiles from 167 profiles available in TIGR3 database. The minimum air temperature at 2 m (the first level),  $T_a$ , is 245 K and the maximum value is 299 K, whereas the water vapour ranges from  $0.2 \text{ g cm}^{-2}$  to  $3.0 \text{ g cm}^{-2}$ .

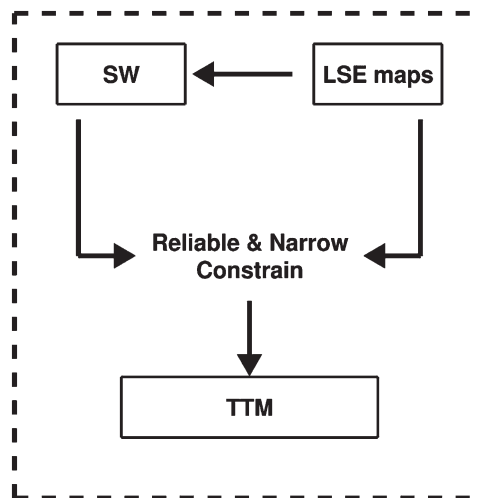


Figure 4. Schematic representation of the hybrid method

Table 6. Impact of the atmospheric correction on the accuracy of the split-window (SW) algorithm for all pairs of AHS bands 75–79 for SZA values of 0 and 60°.

Band		RMSE (K)	
$c_1$	$c_2$	0°	60°
75	76	0.63	1.18
75	77	0.69	1.26
75	78	0.66	1.20
75	79	0.62	1.09
76	77	0.26	0.48
76	78	0.21	0.34
76	79	0.25	0.41
77	78	0.26	0.44
77	79	0.33	0.58
78	79	0.45	0.76

- (2) *LST*: We have considered LST as varying around  $T_a$  from  $T_a - 10.0$  K to  $T_a + 15.0$  K in steps of 5.0 K.
- (3) *LSE*: Based on results from Peres and DaCamara (2005)  $\varepsilon$  was considered as varying from 0.90 to 0.99 in steps of 0.01, and  $\Delta\varepsilon$  as varying from  $-0.01$  to 0.01 in steps of 0.01.

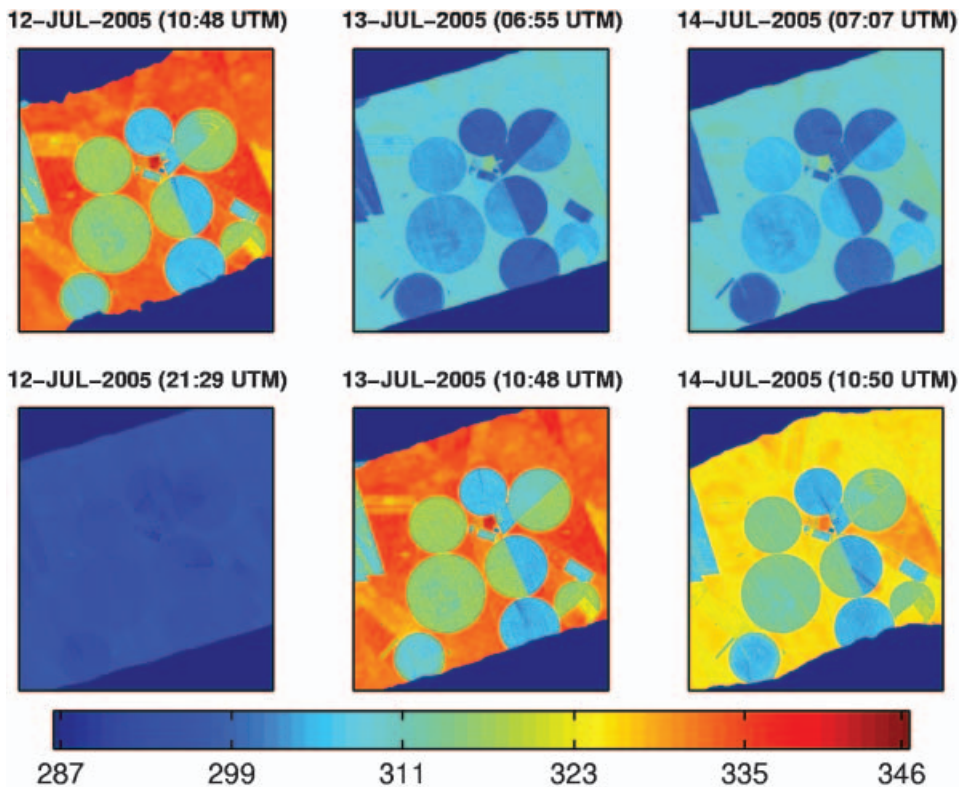


Figure 5. Land surface temperature (LST) retrievals as obtained from the split-window (SW) algorithm, respecting to the first (top) and the second (bottom) Airborne Hyperspectral Scanner (AHS) flights (see table 2) that took place on 12 July 2005 (left panels), 13 July 2005 (middle panels) and 14 July 2005 (right panels). Units of temperature are Kelvin.

- (4) *Satellite zenith angles:* We have selected eight satellite zenith angles (SZAs) covering a range of values from nadir to  $60.0^\circ$ .

Following Sobrino *et al.* (2006) we have computed the SW coefficients  $a_k$  for the 10 possible combinations of two channels  $c_1$  and  $c_2$  (see equation (3)) that were chosen from AHS bands 75–79 and then we have selected the best pair of channels to be used in the SW algorithm. The choice was based on the respective impacts on LST accuracy of the different atmospheric correction schemes. The impact was quantified by the error of the regression models for the different pairs of channels. Results are shown in table 6 for both  $SZA=0^\circ$  and  $SZA=60^\circ$  and the best combination was found for AHS bands 76 and 78. It is worth noting that the database of simulated radiances was constructed by using the whole atmosphere (TIGER3 atmospheric profiles) as input to MODTRAN4, accordingly applying the SW coefficients in equation (3) to correct atmospheric effects from flights at an altitude of 1340 m may introduce errors in LST retrievals. However, the resulting uncertainty in the estimated LST is expected to be small because the database covers a wide variety of geophysical situations (i.e. different atmospheric profiles and geometrical paths) and therefore certainly includes the atmospheric conditions resulting in the thermal radiances observed by the AHS radiometer.

In order to obtain an operational SW algorithm we have also derived a single algorithm that explicitly takes into account the AHS SZA. For this purpose we have derived a set of new coefficients ( $b_{0k}$ ,  $b_{1k}$  and  $b_{2k}$ ) by fitting to a quadratic function of SZA the SW coefficients  $a_k$ , as computed for the eight specific SZAs (ranging from nadir to  $60^\circ$ )

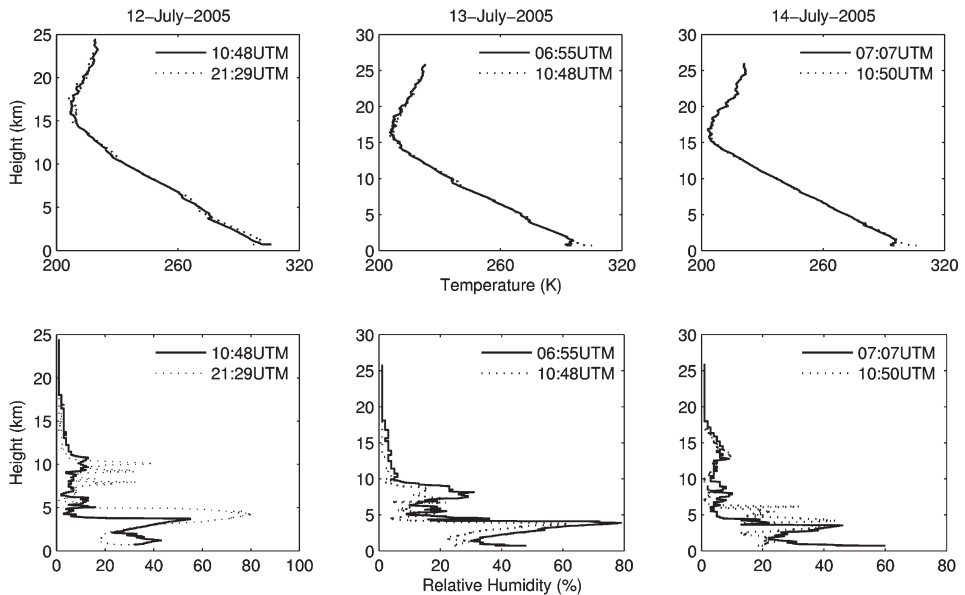


Figure 6. Profiles of temperature (upper panels) and relative humidity (lower panels) from *in situ* atmospheric soundings launched over Barrax test site on 12 July 2005 (left panels), 13 July 2005 (middle panels) and 14 July 2005 (right panels).

$$a_k = b_{0k} + b_{1k} \cos(\text{SZA}) + b_{2k} \cos(\text{SZA})^2 \quad (4)$$

Finally the performance of the hybrid method was tested under the assumption of the (least favourable) general case where LSE is not well known *a priori* in the study area. Accordingly, we have assigned laboratory measurements of LSE (as obtained from the Johns Hopkins University (JHU) Spectral Library) to the GLC2000 Land Cover map (see figure 1), which has a 1-km nominal spatial resolution. GLC2000 classifies the whole area of the Barrax test site as Cultivated/Managed Areas and taking into account that soils of the molisol-type tend to be base rich and quite fertile, and being the best agricultural soil, this class was characterized in a rather simple way by assuming the following samples and weights: 50% of green grass+50% of molisols. The prescribed LSE values for channels 76 and 78 are 0.976 and 0.980, respectively.

LST retrievals respecting to the above-mentioned prescribed LSE values for channels 76 and 78 were derived with the developed SW algorithm and obtained results are shown in figure 5 for the AHS flights over the Barrax test site.

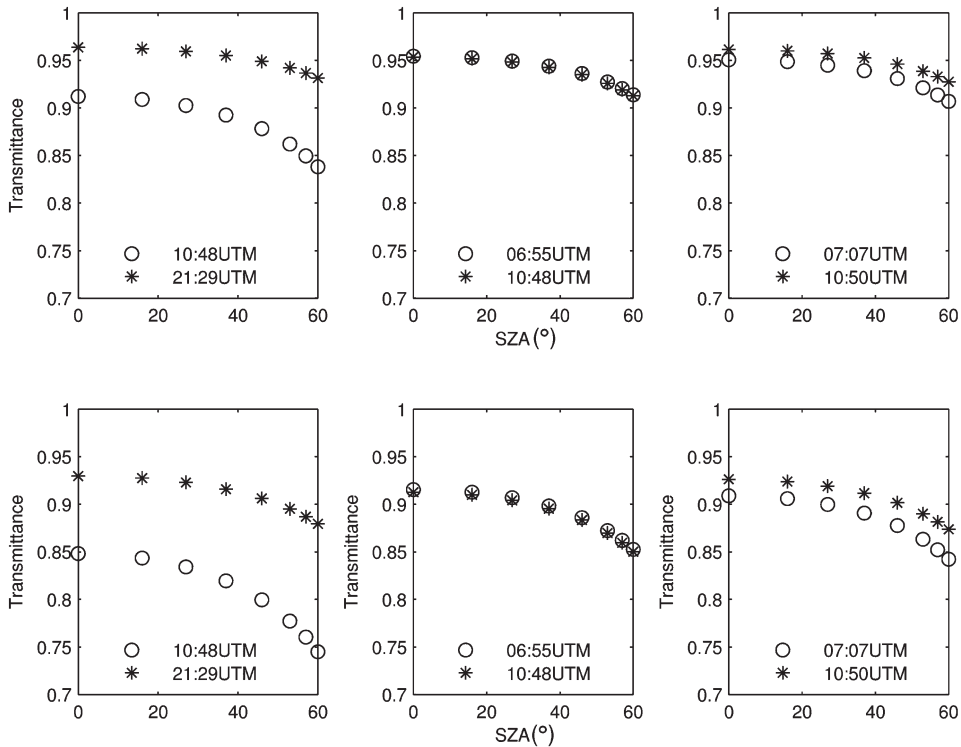


Figure 7. Values of atmospheric transmittance in Airborne Hyperspectral Scanner (AHS) bands 76 (upper panels) and 78 (lower panels) for eight selected satellite zenith angles (SZAs) as computed with MODTRAN4 from atmospheric soundings launched over Barrax test site on 12 July 2005 (left panels), 13 July 2005 (middle panels) and 14 July 2005 (right panels).

#### 4.2 Atmospheric correction

As described in §1 the proposed hybrid method is an emissivity-temperature separation algorithm and therefore it requires temperature and humidity atmospheric profiles as inputs to a RTM in order to perform the atmospheric correction. Accordingly, the atmospheric correction was carried out based on the RTE given by equation (1), where the atmospheric parameters, i.e. the atmospheric transmittance  $\tau_c(\theta)$  and the atmospheric upwards and downwards radiances  $L_c^\uparrow(\theta)$  and  $L_c^\downarrow$ , were computed using MODTRAN4 and the *in situ* atmospheric soundings (see figure 6), which were launched almost simultaneously to the AHS flights. The atmospheric parameters in AHS bands 76 and 78 were finally obtained (see figure 7 for transmittance) using the response functions of the AHS bands 76 and 78 (see figure 3) for the same eight SZA values considered in the SW algorithm. In order to atmospherically correct the whole area imaged by the AHS instrument, i.e. including those pixels with different SZAs from the eight considered values, we have adopted the same procedure used in the SW algorithm and have expressed the atmospheric parameters as a quadratic function of SZA. Figures 8 and 9 show respectively the transmittance in AHS bands 76 and 78 for the AHS SZA images as computed by the above-mentioned procedure.

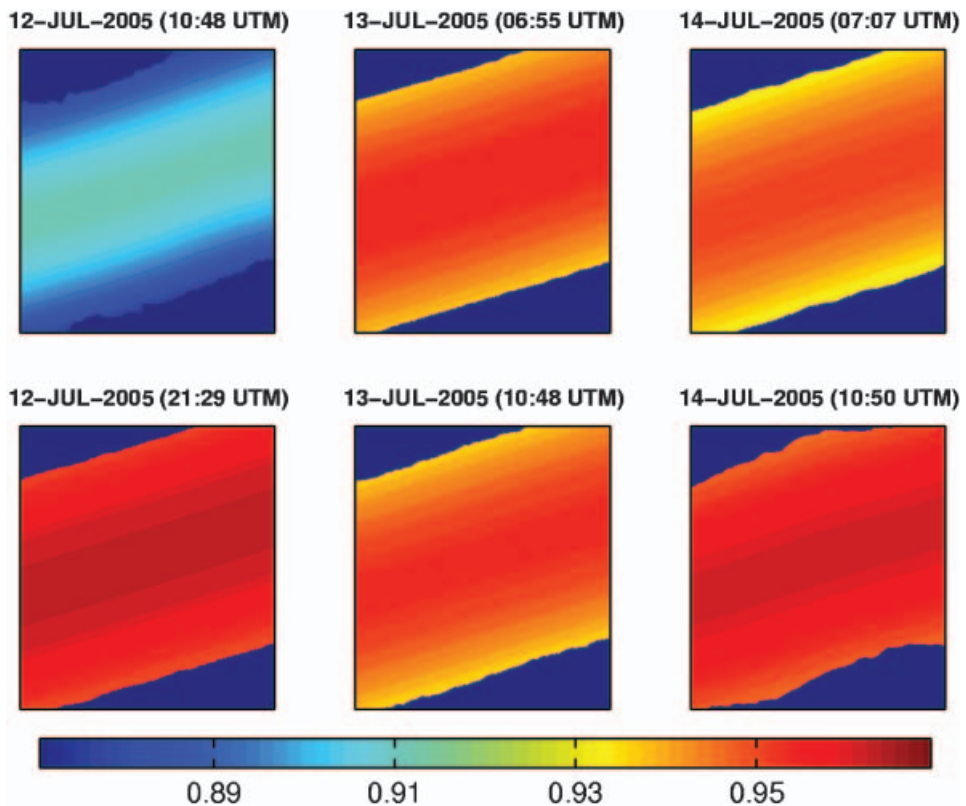


Figure 8. Atmospheric transmittance in the Airborne Hyperspectral Scanner (AHS) band 76 for the study area of Barrax computed from atmospheric soundings and spatially interpolated based on satellite zenith angle information from AHS images acquired on 12 July 2005 (left panels), 13 July 2005 (middle panels) and 14 July 2005 (right panels).

It is worth mentioning at this point that the thermal radiometers that were described in §2 are used at ground-level and measure in fact the land-leaving radiance  $L_{LLR_c}$  (Sobrino *et al.* 2006)

$$L_{LLR_c} = \epsilon_c B_c(T_s) + L_c^\downarrow(1 - \epsilon_c) \tag{5}$$

where equation (5) may be derived from equation (1) under the assumptions that  $\tau_c(\theta) \approx 1$  and  $L_c^\uparrow(\theta) \approx 0$  at ground-level. Accordingly, we have found the value of  $T_s$  from ground-based measurements by taking into account both LSE and atmospheric effects on the radiance as measured with the thermal radiometers. LSE values were measured *in situ* using both the box method and the TES algorithm, whereas the atmospheric downwards radiance was computed using atmospheric soundings as input to MODTRAN4. In order to illustrate the difference between surface temperature  $T_s$  and the radiometric temperature  $T_{rad}$  (i.e. the temperature obtained when Planck’s law is inverted using the land-leaving radiance  $L_{LLR_c}$ ), Sobrino *et al.* (2006) have shown examples of estimates of  $T_s$  and  $T_{rad}$  as obtained with thermal radiometers over bare soil and grass in the Barrax test site. Differences between  $T_s$  and  $T_{rad}$  were around 2 K for bare soil and 1 K for grass.

### 4.3 The hybrid method

In order to assess the improvements on LST and LSE estimations allowed by the proposed hybrid method, we have considered the two following cases: (1) SW is used

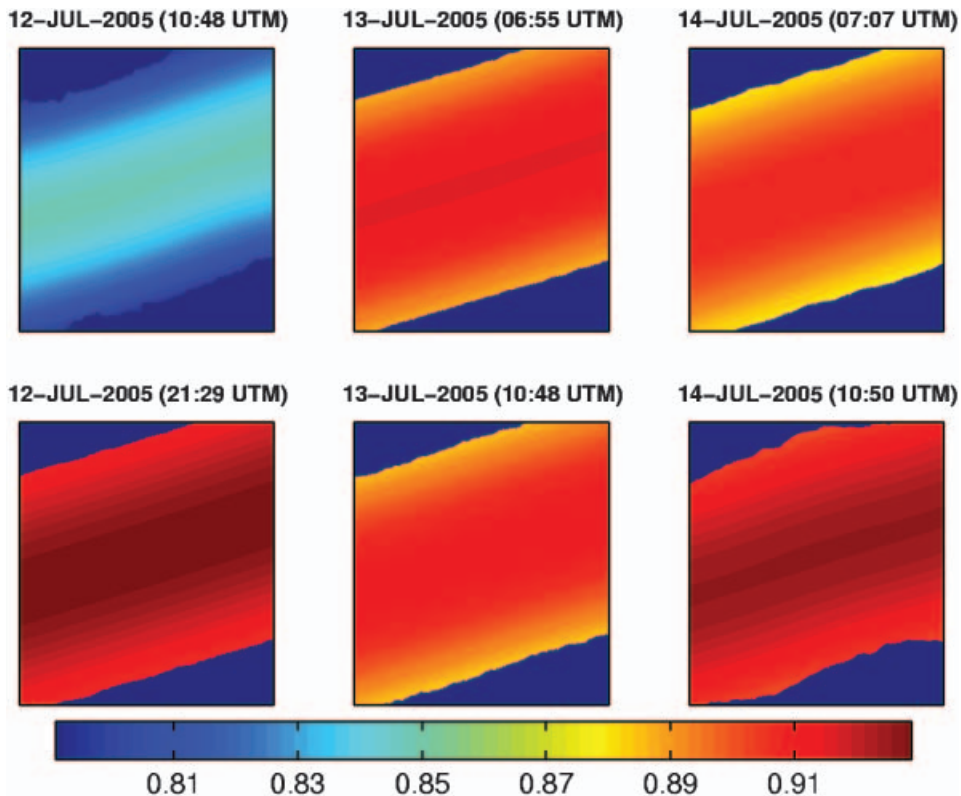


Figure 9. As in figure 8, but for the Airborne Hyperspectral Scanner (AHS) band 78.

alone and (2) the new hybrid method is applied. Results respecting to the single usage of SW are shown in figure 5 for AHS flights, whereas those obtained using the hybrid method are shown in figures 10 and 11 for LST and LSE retrievals, respectively.

#### 4.4 Comparison with in situ measurements

We have computed the differences between AHS-retrieved temperatures respecting to the hybrid method ( $T_s^{\text{HB}}$ ) and the SW algorithm ( $T_s^{\text{SW}}$ ) and *in situ* average temperature measurements ( $T_s^{\text{in situ}}$ ) for each site and scene. Table 7 shows the *in situ* averages of temperature, the corresponding standard deviation ( $\delta$ ) for each site and the differences between the retrieved and the measured temperatures. The last three lines in table 7 show values of bias, standard deviation ( $\delta$ ) and root-mean square error (RMSE) between ground measurements and derived LST using each method for all sites and scenes together. It may be noted that the hybrid method provides LST values with bias (RMSE) of 0.8 K (1.9 K). These figures point out the better performance of the hybrid method and are worth being compared with those obtained when using SW alone, namely the values of 2.7 K (3.4 K) for the bias (RMSE). The above-mentioned results also point out the satisfactory agreement between *in situ* and hybrid method temperatures.

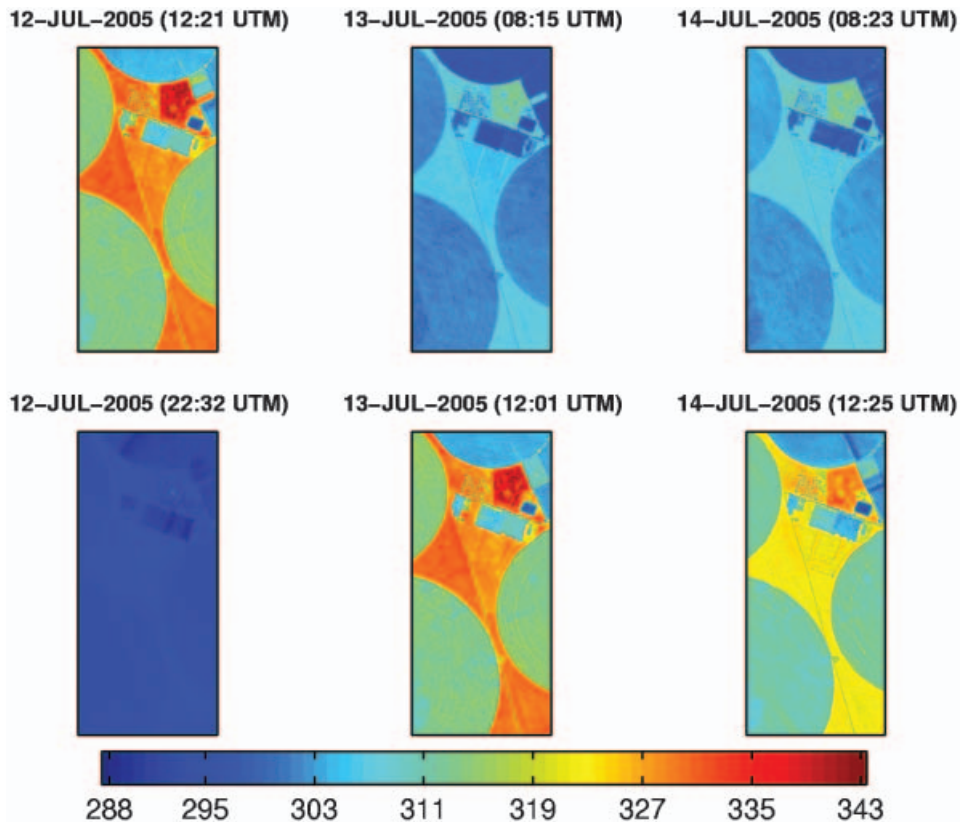


Figure 10. Land surface temperature (LST) retrievals as obtained from the hybrid method respecting to the first (top) and the second (bottom) Airborne Hyperspectral Scanner (AHS) flights (see table 2) that took place on 12 July 2005 (left panels), 13 July 2005 (middle panels) and 14 July 2005 (right panels). Units of temperature are Kelvin.

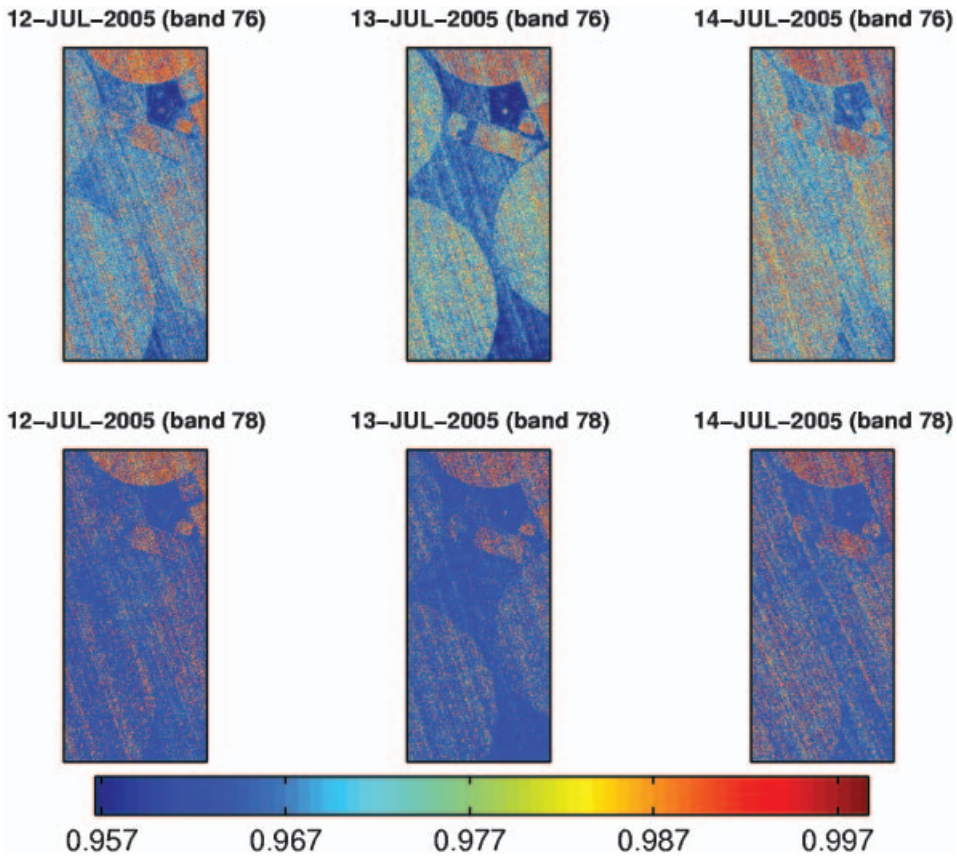


Figure 11. Land surface emissivity (LSE) retrievals as obtained from the hybrid method respecting to Airborne Hyperspectral Scanner (AHS) channels 76 (top) and 78 (bottom) and to the flights of 12 July 2005 (left panels), 13 July 2005 (middle panels) and 14 July 2005 (right panels).

Unlike the SW algorithm, the hybrid method provides LSE retrievals simultaneously to LST. Table 8 shows the comparison between *in situ* LSE measurements ( $\epsilon_c^{\text{in situ}}$ ) and the LSE retrievals from the hybrid method ( $\epsilon_c^{\text{HB}}$ ) for AHS bands 76 and 78. It is worth noting that the hybrid method provides estimates of LSE values with bias (RMSE) of  $-0.008$  (0.013) for channel 76, whereas for channel 78 the corresponding obtained values are  $-0.011$  (0.017).

## 5. Discussion and conclusions

We have validated a new hybrid method based on a synergistic usage of SW and TTM, which combines the attractive features of both methods while mitigating some of their drawbacks. The hybrid method was tested and compared with a SW algorithm using data obtained with an AHS radiometer from flights at an altitude of 1340 m, yielding a pixel resolution of 3.4 m and *in situ* measurements acquired in the framework of the SEN2FLEX campaign. The field campaign was conducted in the Barrax test site (Albacete, Spain) on 12, 13, 14 July 2005, where a set of radiometric measurements were performed in the TIR spectral region for different surface types, e.g. bare soil, water body, corn, wheat, grass. These measurements include surface

Table 7. Results obtained for the land-surface temperature (LST) validation of the hybrid method and the split-window (SW) algorithm.

Site	Scene (date 2005 and UTM)	$T_s^{\text{in situ}}$ (°C)	$\delta$ (°C)	$T_s^{\text{HB}} - T_s^{\text{in situ}}$ (°C)	$T_s^{\text{SW}} - T_s^{\text{in situ}}$ (°C)
BS7 – Bare Soil	12 July 12:21	52.1	1.6	4.4	7.2
	12 July 22:32	20.6	0.7	2.0	2.3
	14 July 08:23	29.3	0.8	4.7	5.9
	14 July 12:25	47.4	1.3	1.9	4.7
L13 – Grass	12 July 12:21	37.8	2.6	-0.5	1.6
	12 July 22:32	18.3	0.9	-0.8	-0.7
	13 July 08:15	25.5	1.4	-0.8	0.9
	13 July 12:07	36.2	0.0	-0.4	2.8
	14 July 08:23	25.5	0.8	0.3	1.8
	14 July 12:25	31.7	1.2	-0.3	1.4
WB – Water	12 July 12:21	23.9	1.2	-0.5	1.6
	12 July 22:32	18.3	1.1	1.8	3.1
	13 July 08:15	20.4	0.8	-0.2	1.7
	13 July 12:07	23.9	0.6	1.4	3.2
	14 July 08:23	20.1	0.8	0.7	2.0
	14 July 12:25	20.1	1.3	2.2	3.9
W1 – Wheat	12 July 12:21	39.3	1.6	-0.7	3.0
	12 July 22:32	21.3	0.3	-0.5	-0.1
SC1 – Corn	12 July 12:21	32.5	3.6	4.6	6.8
	12 July 22:32	20.6	0.5	-0.4	-0.5
	14 July 08:23	24.0	1.7	1.7	2.7
	14 July 12:25	32.2	1.5	-1.0	4.5
Bias				0.8	2.7
$\delta$				1.8	2.1
RMSE				1.9	3.4

temperature in coincidence with aircraft overpasses using different thermal radiometers, thermal angular measurements using a goniometric motorized system, thermal imagery with two thermal cameras and emissivity measurements using the box method and the TES algorithm. The atmospheric correction of the AHS TIR channels was performed based on humidity and temperature profiles from radiosounding measurements carried out almost simultaneously to the AHS overpass, which were then used as input to MODTRAN4.

In order to build up a suitable SW algorithm for the AHS instrument, we have performed radiative transfer simulations for different geophysical conditions. In addition, we have investigated the best combination of AHS bands 75–79 to be used in the SW algorithm and found bands 76 and 78 to be the best pair. With the aim of obtaining an operational SW algorithm for LST retrievals from AHS imagery, we have also derived a single algorithm that explicitly takes into account the AHS SZA.

The performance of the hybrid method was tested by assuming a general case where LSE in AHS bands 76 and 78 are not well known *a priori* over the study area. Accordingly, we have assigned laboratory measurements of LSE to the GLC2000 Land Cover map, which classifies the whole area of the Barrax test site as Cultivated/Managed Areas.

The hybrid method has retrieved LST values with bias (RMSE) of 0.8 K (1.9 K). These figures point out the better performance of the hybrid method and are worth being compared with those obtained when using SW alone, namely the values of 2.7 K (3.4 K) for the bias (RMSE). Accordingly, the hybrid method was able to

Table 8. Results obtained for the land surface emissivity (LSE) validation of the hybrid method.

Site	Scene (date 2005 and UTM)	$\epsilon_{76}^{\text{in situ}}$	$\epsilon_{76}^{\text{HB}} - \epsilon_{76}^{\text{in situ}}$	$\epsilon_{78}^{\text{in situ}}$	$\epsilon_{78}^{\text{HB}} - \epsilon_{78}^{\text{in situ}}$
BS7 – Bare Soil	12 July 12:21	0.971	-0.004	0.970	-0.006
	12 July 22:32				
	14 July 08:23		-0.018		-0.024
	14 July 12:25				
L13 – Grass	12 July 12:21	0.986	-0.014	0.988	-0.022
	12 July 22:32				
	13 July 08:15		-0.007		-0.018
	13 July 12:07				
	14 July 08:23		-0.016		-0.019
WB – Water	14 July 12:25				
	12 July 12:21	0.995	-0.010	0.993	-0.016
	12 July 22:32				
	13 July 08:15		-0.013		-0.019
	13 July 12:07				
W1 – Wheat	14 July 08:23		-0.018		0.018
	14 July 12:25				
	12 July 12:21	0.960	0.013	0.951	0.015
SC1 – Corn	12 July 22:32				
	12 July 12:21	0.987	-0.012	0.988	-0.017
Bias	12 July 22:32				
	14 July 08:23		0.011		-0.015
	14 July 12:25				
$\delta$			-0.008		-0.011
RMSE			0.010		0.013
			0.013		0.017

provide estimates of LST with values of bias (RMSE) about one third (one half) of the corresponding values that were obtained with the SW algorithm. The above-mentioned results indicate a satisfactory agreement between *in situ* and hybrid method temperatures.

The proposed new hybrid method seems therefore to provide better results than those from the single usage of SW and this is especially true in the case of atmospheric profiles characterized by a lower water vapour content (please see the values of transmittance in figures 7–9). However, this may be not true in the case of very wet atmospheres since previous studies (e.g. Wan and Dozier 1996) have shown that it is not necessary to know LSE with high accuracy for wet atmospheres as the sensitivity of SW to LSE decreases as the atmospheric water vapour content increases. This is due to the fact that the emissivity effect on the emitted surface radiance is largely compensated by the downwards atmospheric TIR radiance that is reflected by the surface. Conversely, for dry conditions the LST error due to uncertainties in LSE may be quite significant.

In respect to LSE, obtained results show that the hybrid method is capable of estimating LSE values with bias (RMSE) of -0.008 (0.013) for channel 76, whereas for channel 78 the corresponding obtained values were -0.011 (0.017).

In summary, the hybrid method has shown to be adequate to retrieve LST for areas where LSE is highly variable and not well known *a priori* and provide a sound indication that the developed approach is particularly useful for surface and atmospheric conditions where SW algorithms cannot be accurately applied.

### Acknowledgments

The research was performed within the framework of the Project Satellite Application Facility on Land Surface Analysis (LSA-SAF), an R&D Project sponsored by EUMETSAT. The ASTER spectral library was available courtesy of the Jet Propulsion Laboratory, California Institute of Technology, Pasadena, California.

### References

- ALIX, F.-R., GÓMEZ, J.A. and MIGUEL, E., THE INTA AHS SYSTEM, 2005, Sensors, systems, and next-generation satellites IX. *Proceedings of the SPIE*, **5978**, pp. 471–478.
- BECKER, F., 1987, The impact of spectral emissivity on the measurement of land surface temperature from satellite. *International Journal of Remote Sensing*, **8**, pp. 1509–1522.
- BERK, A., ANDERSON, G.P., ACHARYA, P.K., CHETWYND, J.H., BERNSTEIN, L.S., SHETTLE, E.P., MATTHEW, M.W. and ALDER-GOLDEN, S.M., 2000, MODTRAN4 version 2 user's manual. Air Force Research Laboratory, Space Vehicles Directorate, Air Force Material Command, Hanscom AFB, MA 01731-3010.
- FAYSASH, A. and SMITH, E.A., 2000, Simultaneous retrieval of diurnal to seasonal surface temperatures and emissivities over SGP ARM-CART site using GOES split window. *Journal of Applied Meteorology*, **39**, pp. 971–982.
- GILL, P.E., MURRAY, W. and WRIGHT, M.H., 1983, *Practical Optimization* (New York: Academic Press).
- GILLESPIE, A.R., ROKUGAWA, S., HOOK, S.J., MATSUNAGA, T. and KAHLE, A.B., 1999, Temperature/emissivity separation algorithm theoretical basis document. Version 2.4. Jet Propulsion Laboratory, Pasadena. Prepared under NASA Contract NAS5-31372. Available online at: [http://eosps0.gstc.nasa.gov/eos\\_homepage/for\\_scientists/atbd/docs/ASTER/atbd-ast-05-08.pdf](http://eosps0.gstc.nasa.gov/eos_homepage/for_scientists/atbd/docs/ASTER/atbd-ast-05-08.pdf) (accessed 4 August 2008).
- NERRY, F., LABED, J. and STOLL, M.P., 1990, Spectral properties of land surfaces in the thermal infrared band: Part II. Field method for spectrally averaged emissivity measurements. *Journal of Geophysical Research*, **95**, pp. 7027–7044.
- PERES, L.F. and DACAMARA, C.C., 2004, Land surface temperature and emissivity estimation based on the Two-Temperature Method: sensitivity analysis using simulated MSG/SEVIRI data. *Remote Sensing of Environment*, **91**, pp. 377–389.
- PERES, L.F. and DACAMARA, C.C., 2005, Emissivity maps to retrieve land-surface temperature from MSG/SEVIRI data. *IEEE Transactions on Geoscience and Remote Sensing*, **45**, pp. 1834–1844.
- PERES, L.F. and DACAMARA, C.C., 2008, Improving the retrieval of land surface temperature with a synergistic use of the two-temperature and the split-window methods. *Remote Sensing of Environment* (submitted).
- SOBRINO, J.A. and RAISSOUNI, N., 2000, Toward remote sensing methods for land cover dynamic monitoring. Application to Morocco. *International Journal of Remote Sensing*, **20**, pp. 353–366.
- SOBRINO, J.A., JIMÉNEZ-MUÑOZ, J.C., ZARCO-TEJADA, P.J., SEPULCRE-CANTÓ, G. and DE MIGUEL, E., 2006, Land surface temperature derived from airborne hyperspectral scanner thermal infrared data. *Remote Sensing of Environment*, **102**, pp. 99–115.
- WAN, Z. and DOZIER, J., 1996, A generalised split-window algorithm for retrieving land-surface temperature from space. *IEEE Transactions on Geoscience and Remote Sensing*, **34**, pp. 892–905.